(Submitted to
PHYSICS OF FLUIDS)

A STATISTICAL FORMULATION OF ONE-
DIMENSIONAL ELECTRON FLUID TURBULENCE

By

David Fyfe[*] and David Montgomery

Department of Physics and Astronomy
The University of Iowa
Iowa City, Iowa 52242

June 1977

[*]Current Address: Department of Computer Science
Yale University
New Haven, Connecticut 06520

A STATISTICAL FORMULATION OF ONE-

DIMENSIONAL ELECTRON FLUID TURBULENCE

By

David Fyfe* and David Montgomery

Department of Physics and Astronomy
The University of Iowa
Iowa City, Iowa 52242

June 1977

*Current Address: Department of Computer Science
Yale University
New Haven, Connecticut 06520

ABSTRACT

A one-dimensional electron fluid model is investigated using
the mathematical methods of modern fluid turbulence theory. Non-
dissipative equilibrium canonical distributions are determined in a
phase space whose co-ordinates are the real and imaginary parts of
the Fourier coefficients for the field variables. Spectral densities
are calculated, yielding a wavenumber electric field energy spectrum
proportional to k^{-2} for large wavenumbers. The equations of motion
are numerically integrated and the resulting spectra are found to
compare well with the theoretical predictions.

I. INTRODUCTION

Though not yet a completed program, the statistical theory of fluid turbulence has made remarkable strides in the last two decades. Many of these advances have not been digested by the plasma turbulence community, however. Plasma turbulence theory, consequently, has developed in a considerably less convincing conceptual framework and has achieved less detailed verification of its predictions in experiment and numerical simulation than fluid turbulence has.

It is of interest to see how many turbulent plasma situations can be treated by methods borrowed from fluid turbulence theory. Though no survey of the plasma turbulence literature is attempted here, we remark upon some recent treatments of incompressible magneto-hydrodynamic turbulence[1-7] in both two and three dimensions. The present article concerns a <u>compressible</u> situation: the electrostatic turbulence of an electron fluid plasma model. The challenging problem of the Vlasov plasma, despite its enormous literature, does not appear to us to be quite ripe for an approach through modern turbulence techniques, except possibly in the so-called "weak turbulence" limit, which has been extensively studied.

The principal concern in fluid turbulence has been with high Reynolds number situations. For these, the nonlinear terms are so much larger than the linear ones that the dominant physical effect

can be accurately said to be the transfer of the excitations from one spatial scale to another. Often, migrations of energy across orders of magnitude in spatial scale are involved. These migrations can be toward either shorter or longer wavelengths, depending upon the circumstances. There is an accompanying emphasis in the theory on the wavenumber spectrum, on energy transfer functions, on cascades through wavenumber space, and so on. An unanswered question (almost an unasked one) in electrostatic plasma turbulence concerns the extent to which the phenomena also involve large migrations of energy from one spatial scale to another. With few exceptions, theories have been formulated in ways that implicitly assume that no such migrations occur, and provide no mathematical machinery to describe the transfer. Numerical simulations typically have not involved sufficiently fine spatial resolution to see such migrations, and the intensity of the search for a stable, quiescent equilibrium has often led simulators to stop computing as soon as spatial fine structure has begun to develop. Spectral-method computing techniques,[8-11] which are well suited to computing simultaneously on a wide range of spatial scales in Navier-Stokes and magnetohydrodynamic fluids, have not yet had much impact on plasma simulation. Configuration-space computations are less than satisfactory for following evolving turbulent fields.

There are some good reasons for the neglect. Plasmas do not obey the same dynamical equations over as many orders of magnitude

in spatial scale as Navier-Stokes fluids or·stellar-interior MHD fluids typically do. For example, while MHD fluid descriptions may satisfactorily represent the largest-scale dynamics of a tokamak plasma, on the scale of the ion gyroradius there are important phenomena which are not contained in MHD at all. The incorporation of quite different mathematical descriptions within the calculation of a single turbulent situation lies out of reach of known procedures. All this implies that most situations about which we can make logically compelling quantitative assertions will be "unrealistic" in the sense that they will omit phenomena of importance for real experiments. One of two alternatives must be chosen: (1) continue to ignore the possibility that interesting plasmas are, like other fluids, turbulent in a sense that involves transfer of the energy in the field from one spatial scale to another; or (2) study highly simplified models that, while certain never to tell the whole story about a turbulent plasma, may at least tell a part of it accurately. In the present article we opt for the second choice as being historically the more likely one along which progress may be expected.

In Sec. II we present the details of the model of an electron plasma to be studied. It is important to recognize that in restricting attention to an electron plasma with uniform immobile ions, we will be omitting one of the more popular phenomena of the day: "Langmuir solitons", and other related situations in which the ponderomotive force is involved in a fundamental way. In Sec. III the statistical-

mechanical predictions are derived. Section IV is a presentation of some preliminary numerical tests of the material presented in Sec. III. Section V summarizes and discusses the results.

II. THE MODEL

We take the simplest possible model in which electrostatic effects in a plasma will be exhibited: the one-dimensional electron plasma with a locally adiabatic equation of state. If the electron density is n, the fluid velocity is v, the electric field is E, and the ratio of specific heats γ is 2, we have, in dimensionless units,

$$\frac{\partial n}{\partial t} + \frac{\partial}{\partial x} (nv) = 0 \quad , \tag{1}$$

$$\frac{\partial v}{\partial t} + v \frac{\partial v}{\partial x} = -E - \frac{\partial n}{\partial x} + \nu \frac{\partial^2 v}{\partial x^2} \quad , \tag{2}$$

$$\frac{\partial E}{\partial x} = 1 - n \quad . \tag{3}$$

We may replace Poisson's equation, Eq. (3), by

$$\frac{\partial E}{\partial t} = nv \tag{4}$$

which is an equation for the time advancement for the electric field, if we invoke Poisson's equation as an initial condition. Equations (1), (2), and (4) will then preserve the Poisson relation in time.

n, E, and v in Eqs. (1)—(4) are functions of only one space coordinate x, and the time t. n is measured in units of n_o, the equilibrium average number density of the electrons and (immobile) positive ion background. Times are measured in units of the inverse electron plasma frequency ω_{pe}^{-1}, and velocities in units of the electron thermal velocity; lengths are in units of the Debye length. The mechanical pressure gradient enters in the second term on the right-hand side of Eq. (2). Any relation between the pressure and density other than (p/n^2) = constant would have complicated the pressure gradient term in Eq. (2), but we believe that no qualitative restrictions are introduced in the physics by this particular choice of $\gamma = 2$. The term ν is a dimensionless viscosity which can be thought of as the reciprocal of a large Reynolds number. The limit $\nu = 0$ will be called the "non-dissipative" limit, and is the only limit in which Eqs. (1)—(4) are a conservative system. [A linear term proportional to v and containing a collision frequency is also possible in Eq. (2).]

There are typically two standard situations in which the possibility of a tractable steady-state statistical theory of the Navier-Stokes equation has existed: (1) the non-dissipative initial value problem; and (2) the driven, dissipative, steady-state problem in which some external agency supplies energy at a given spatial scale while dissipation occurs at some shorter spatial scale as a consequence of viscosity. The second problem is much more physically realistic than the first, but valuable insights are obtained from studying the

non-dissipative problem as a preliminary. If we want to study the driven, dissipative case for Eqs. (1)—(4), it is necessary to add to the right-hand side of Eq. (2) a driving term which represents an external source of the excitations, and to allow ν to be non-zero.

The really new feature present in Eqs. (1)—(4) which to our knowledge has not yet been incorporated into either MHD or Navier-Stokes theories is the finite compressibility. Incompressibility has been a useful simplifying feature of Navier-Stokes and MHD fluids as far as turbulence goes, but its introduction into a one-dimensional plasma model would render the model meaningless. Compression is essential for electrostatic fields to fluctuate, since they are generated by density inhomogeneities.

That some qualitatively new and unanticipated features are to be expected as a consequence of the finite compressibility can be seen by looking at the right-hand side of Eq. (2) when $\nu = 0$. Compare the two surviving terms with respect to order of magnitude, for an excitation of typical wavenumber k. For a given perturbation of the density of magnitude δn_k, say, Poisson's equation tells us that the magnitude of the electric field to be expected is $\sim \delta n_k/k$. The magnitude of the pressure gradient term, on the other hand, will be $\sim k \delta n_k$. Thus at very long wavelengths ($\gg$ a Debye length) the pressure gradient term will be negligible, while at very short wavelengths ($\ll$ a Debye length) the electric field will be negligible. The excitations will go from being very like a nonlinear cold plasma

oscillation at long wavelengths to very like a nonlinear sound wave at short wavelengths, with a continuous transition in the spatial scales of the order of a Debye length. (This is one respect where the behavior of the model will differ sharply from that of the Vlasov plasma, which, lacking collisions, will also lack the coherence at short wavelengths to exhibit the sound waves.)

The short wavelength behavior of Eq. (2), then, should be that of the Euler equations of a compressible perfect gas. Compressible turbulence usually occurs in gases as a perturbation on incompressible turbulence, and has been studied in isolation very little. One thing our experience with the Euler equations of compressible flow strongly suggests as a possibility, however, is a tendency toward the formation of shocks, or discontinuities. A picture is suggested in which long-wavelength turbulent plasma oscillations feed short-wavelength sound waves, which steepen towards the development of shocks, which in turn are eaten away by the action of the dissipation. The shocks may be very weak ones, and it is imaginable that dissipation might destroy them before their formation becomes complete.

This is a gross, highly conjectural picture for the short wavelength behavior, but is reminiscent of that which is known to occur for Burgers' equation.[12-14] [Burgers' equation is just Eq. (2) minus the first two terms on the right-hand side.] Our program here is to first apply the statistical methods of turbulence theory to the non-dissipative limit of Eqs. (1)—(4), and then to test some of our

predictions by numerical solutions. ˙Inclusion of finite dissipation is a larger matter, and is deferred to a later publication.

III. STATISTICAL FORMULATION

We impose periodic boundary conditions over a length L and Fourier-decompose, in a plane-wave expansion, v, n, and E:

$$v = \Sigma_k \, v(k, \, t) \, \exp \, (ikx) \quad ,$$

$$n = \Sigma_k \, n(k, \, t) \, \exp \, (ikx) \quad ,$$

$$E = \Sigma_k \, E(k, \, t) \, \exp \, (ikx) \tag{5}$$

where Σ_k is over all wave numbers $2\pi m/L$, with $m = 0, \pm 1, \pm 2, \ldots$ It is essential for complete generality to include $m = 0$. It can be shown that $n(k = 0, \, t) = \text{constant} = 1$, but it is not true that we can automatically set $E(k = 0, \, t) = 0$ or $v(k = 0, \, t) = 0$. It is a common belief that the option of setting the $k = 0$ components of E and v identically zero is the only option available or the most natural and acceptable one. Appendix A is devoted to clarifying and correcting this widespread misconception.

The equations for the Fourier coefficients are (with time arguments suppressed for economy)

$$\frac{\partial n(k)}{\partial t} + ik \sum_{p+r=k} n(r) \, v(p) = 0 \quad , \tag{6}$$

$$\frac{\partial v(k)}{\partial t} + \frac{ik}{2} \sum_{p+r=k} v(r) \, v(p) = -E(k) - ikn(k) \quad , \tag{7}$$

$$ikE(k) = -n(k) \quad . \tag{8}$$

Equations (6) and (7) hold for all k. Equation (8), however, holds only for $k \neq 0$. The use of Eq. (8) will eliminate $E(k)$ in favor of $n(k)$ for $k \neq 0$, but an equation is needed $E(0)$. From Eq. (4)

$$\frac{\partial E(0)}{\partial t} = \sum_{k} n(k) \, v(-k) \quad . \tag{9}$$

Equations (6)—(9) are, in general, an infinite set of ordinary differential equations for the Fourier coefficients in the infinite Fourier series and as such are intractable. If further progress is to be made, some simplification has to be made. The simplification made in a linearized theory would be to replace the convolution sums in Eqs. (6) and (7) with the two terms where either $p = 0$ or $r = 0$, thus eliminating all Fourier coefficients from the equations except those with wavenumbers k and 0. The resulting equations are then easily solved. Basically the assumption in the linearized theory is that all non-zero wavenumber Fourier coefficients are small compared to the zero wavenumber Fourier coefficient $n(0)$. The very nature of strong turbulence, however, does not allow one to make this approximation. The standard practice in fluid turbulence is rather to

truncate the Fourier series at a large, but finite, wavenumber k_{max}.
This truncation can be reasonably justified for the dissipative
problem. In that situation one envisions taking k_{max} so large that
for any wavenumbers larger than k_{max}, dissipation wipes out any
Fourier coefficient before it attains any significant value. This
is not true, however, in the non-dissipative limit. Nevertheless
insights into how the nonlinear terms act to shuffle energy between
the various length scales can be obtained through this truncation
just as these insights are gained in the Navier-Stokes and MHD
problems.

The difficulties encountered in trying to solve the large, but
finite, truncated system of equations is not significantly different
from those encountered in the dynamics for a large, but finite,
system of point particles (also described by ordinary differential
equations) in statistical mechanics. In a sense, what we intend to
do here is a statistical mechanics of Fourier coefficients.[15] In a
phase space consisting of the real and imaginary parts of independent
Fourier coefficients we can write down a Liouville equation and ask
for a stationary solution. As we know from elementary statistical
mechanics, such solutions depend critically upon the "constants of
the motion." We have discovered three conserved quantities for Eqs.
(6)—(9). Two of them are the energy $\mathcal{E}$ and the current (or momentum)
J, which in terms of the Fourier coefficients are

$$\mathcal{E} = \frac{1}{2} \sum_{k_1 k_2 k_3 \neq 0} \delta(k_1 + k_2 + k_3) \, n(k_1) \, v(k_2) \, v(k_3)$$

$$+ \frac{1}{2} \sum_{k \neq 0} |v(k)|^2 + \frac{1}{2} \sum_{k \neq 0} |n(k)|^2 + \frac{1}{2} \sum_{k \neq 0} |E(k)|^2 \quad , \quad (10)$$

$$\dot{J} = \sum_{k \neq 0} n(k) \, v(-k) \quad . \tag{11}$$

Notice that the total current (momentum) is not conserved in time, but only the current associated with the $k \neq 0$ modes. $\delta(k_1 + k_2 + k_3)$ in the first term of $\mathcal{E}$ is a Kronecker delta which has the value 1 whenever $k_1 + k_2 + k_3 = 0$ and the value 0 whenever $k_1 + k_2 + k_3 \neq 0$. As a result the first sum in $\mathcal{E}$ is a sum over all sets of three wavenumbers with $0 < |k_i| \leq k_{max}$, $i = 1, 2, 3$ allowed by the periodic boundary conditions which add to zero. This first term we will colloquially call the "triples". The remaining sums in $\mathcal{E}$ and the only sum in J are over all wavenumbers allowed by the periodic boundary conditions with $0 < |k| \leq k_{max}$. To our knowledge $\mathcal{E}$ is the first non-quadratic constant of the motion for a truncated Fourier system to appear in a turbulence calculation. (See Appendix B.)

The constancy of the current reduces the equations for the $k = 0$ Fourier coefficients to a pair of linear equations

$$\frac{\partial v(0)}{\partial t} = -E(0) \quad , \tag{12}$$

$$\frac{\partial E(0)}{\partial t} = v(0) + J \qquad (13)$$

where $n(0) = 1$ has been used. As a result

$$Q = [E(0)]^2 + [v(0) + 2J] \, v(0) \qquad (14)$$

is also a conserved quantity. Equations (12) and (13) have the exact solutions

$$v(0) = -J + (v_o + J) \cos t - E_o \sin t \quad , \qquad (15)$$

$$E(0) = (v_o + J) \sin t + E_o \cos t \qquad (16)$$

where v_o and E_o are the initial values of $v(0)$ and $E(0)$, respectively.

We believe that $\mathcal{E}$, J, and Q are the only conserved quantities which survive the truncation of Eqs. (5)—(9) to a large, but finite, number of Fourier coefficients. A condition that we cannot show and do not believe is true is that the number density $n(x, t)$ formed from the finite Fourier series will remain non-negative at all configuration space points for all time even though the initial number density was non-negative at all points. It would not be totally surprising that a truncated Fourier series would yield a non-physical number density after a finite time in the non-dissipative limit.

The quantities which receive the most attention in turbulence calculations are the wavenumber energy spectra. These spectra here can be calculated as moments of a canonical ensemble constructed in the usual manner from the conserved quantities with an inverse temperature (Lagrange multiplier) for each conserved quantity. Unfortunately the triples make the calculation of moments using the full canonical distribution impossible. We, therefore, consider a "weak turbulence" limit in which the product of three Fourier coefficients can be considered small compared to products of two coefficients. If ε^* represents ε without the triples and $Q^* = [E(0)]^2 + [v(0)]^2$ then we propose to use the canonical distribution

$$D = \eta \, \exp \, (-\alpha \varepsilon^* - \beta J - \gamma Q^*) \tag{17}$$

to calculate the moments of Fourier coefficients. η is a normalizing constant determined by the normalization

$$\int D \, dX = 1 \tag{18}$$

where $\int dX$ is an integral over all the independent real and imaginary parts of Fourier coefficients. Since $n(k) = n^*(-k)$ and $v(k) = v^*(-k)$, independent Fourier coefficients are associated with only half the wavenumbers. Furthermore $E(k)$ and $n(k)$ for $k \neq 0$ are not independent since they are related through Poisson's equation. α, β, and γ play

the role of inverse temperatures and are constained by the requirement that D be normalizable.

We can make a further simplification. Q^* involves only the k = 0 modes while E^* and J involve only modes with $k \neq 0$. Since we already have exact solutions for the k = 0 modes and are interested in expectation values for the energy in the $k \neq 0$ modes we can use, for the purposes of the calculation

$$D = \eta \exp (-\alpha \mathcal{E}^* - \beta J) \tag{19}$$

Furthermore, since $\mathcal{E}^*$ and J are sums of terms indexed by a single wavenumber, D factors into a product of distribtuions, one for each k. The single-k distribution is

$$f_k[n_r(k),\ n_i(k),\ v_r(k),\ v_i(k)]$$

$$= \eta_k \exp \left(-\alpha \left\{ v_r^2(k) + v_i^2(k) + \left[1 + \frac{1}{k^2} \right] \left[n_r^2(k) + n_i^2(k) \right] \right\} \right.$$

$$\left. - 2\beta [n_r(k)\ v_r(k) + n_i(k)\ v_i(k)] \right) \tag{20}$$

where $n(k) = n_r(k) + i n_i(k)$ and $v(k) = v_r(k) + i v_i(k)$. The normalizing constants are given by

$$\eta_k = \frac{\alpha}{\pi^2} \left[\alpha \left(1 + \frac{1}{k^2} \right) - \frac{\beta^2}{\alpha} \right] \quad . \tag{21}$$

The requirements that the distributions be normalizable are that

$$\alpha > 0 \quad ,$$

$$\tag{22}$$

$$\alpha \left(1 + \frac{1}{k^2} \right) - \frac{\beta^2}{\alpha} > 0 \qquad \text{for all } k.$$

The latter condition can be met for all k if it can be satisfied for k_{max}.

Expectation values can now be computed.

$$\langle n_r^2(k) \rangle = \langle n_i^2(k) \rangle = \frac{1}{2} \frac{1}{\left[\alpha \left(1 + \frac{1}{k^2} \right) - \frac{\beta^2}{\alpha} \right]} \quad , \tag{23}$$

$$\langle v_r^2(k) \rangle = \langle v_i^2(k) \rangle = \frac{1}{2} \left\{ \frac{1}{\alpha} + \frac{\frac{\beta^2}{\alpha^2}}{\left[\alpha \left(1 + \frac{1}{k^2} \right) - \frac{\beta^2}{\alpha} \right]} \right\} , \tag{24}$$

$$\langle n_r(k)\, v_r(k) \rangle = \langle n_i(k)\, v_i(k) \rangle = - \frac{\beta}{2\alpha} \frac{1}{\left[\alpha \left(1 + \frac{1}{k^2} \right) - \frac{\beta^2}{\alpha} \right]} \cdot \tag{25}$$

Hence the wavenumber energy spectra are given by

$$\langle |v(k)|^2 \rangle = \frac{1}{\alpha} + \frac{\beta^2}{\alpha^2} \frac{1}{\alpha\left(1 + \frac{1}{k^2}\right) - \frac{\beta^2}{\alpha}} \quad , \tag{26}$$

$$\langle |n(k)|^2 \rangle = \frac{1}{\left[\alpha\left(1 + \frac{1}{k^2}\right) - \frac{\beta^2}{\alpha}\right]} \quad , \tag{27}$$

and

$$\langle |E(k)|^2 \rangle = \frac{1}{k^2\left[\alpha\left(1 + \frac{1}{k^2}\right) - \frac{\beta^2}{\alpha}\right]} \quad . \tag{28}$$

α and β are determined by the condition that the expectation values of ε^* and J match their initial values; that is, α and β are solutions of the algebraic equations

$$\varepsilon^* = \sum_{k \neq 0} \left[\frac{1}{\alpha} + \frac{1}{\alpha} \frac{\alpha(1 + k^2) + \left(\frac{\beta^2}{\alpha}\right) k^2}{\alpha(1 + k^2) - \left(\frac{\beta^2}{\alpha}\right) k^2} \right] \quad , \tag{29}$$

$$J = - \sum_{k \neq 0} \frac{\beta}{\alpha} \frac{k^2}{\alpha(1 + k^2) - \left(\frac{\beta^2}{\alpha}\right) k^2} \quad . \tag{30}$$

The electric field energy spectrum as a function of wavenumber has one basic shape: concave down, proportional to k^{-2} for $k \gg 1$ and approaching the constant value α^{-1} for $k \ll 1$ with a continuous transition region in between.

In the particular case that $J = 0$ we have that $\beta = 0$ and the spectra reduce to the simpler forms

$$\langle |E(k)|^2 \rangle = \frac{1}{\alpha(1 + k^2)} \tag{31}$$

and

$$\langle |v(k)|^2 \rangle = \frac{1}{\alpha} \quad . \tag{32}$$

It is this particular case which we will examine numerically in the following section.

IV.   NUMERICAL RESULTS

Equations (6)—(9) are solved numerically using the spectral method of Orszag and Patterson.[7-10]   The essence of the spectral method is to evaluate the convolution sums which appear in these equations by using the convolution theorem and a Fast Fourier Transform.   Unfortunately the convolution theorem does not recognize truncations in k-space.   Modes with $|k| > k_{max}$ can be generated, leading to what are termed aliasing errors.   We have eliminated these aliasing errors by setting to zero the outer one-third of our computational array at the end of each time step.   That is, if N is the total number of configuration space grid points, we have retained only the $2N/3$ wavenumbers of smallest magnitude out of the possible N Fourier modes by setting $k_{max} = (N/3) k_{min}$ where k_{min} is the smallest non-zero wavenumber allowed by the periodic boundary conditions.

The time advancement is done using a fourth-order Adams-Bashforth-Moulton predictor-corrector with the first two time steps being calculated by a fourth-order Runge-Kutta method.[16]

Table I gives a list of parameters for three typical runs in which there is no initial J and hence $\beta = 0$.   Each run begins with a highly non-thermal equilibrium spectrum and the Fourier coefficients are then followed in time.   The initial loading sets $n(k)$ with $|k| = 6k_{min}$, $7k_{min}$, $8k_{min}$, $9k_{min}$, and $10k_{min}$ initially non-zero and

all other coefficients to zero. The magnitudes of the non-zero

coefficients are given, but the phases are chosen randomly.

Run 2 uses 42 wavenumbers (21 positive and 21 negative) with

magnitudes which lie predominantly above $k = 1$. Run 3 consists of

42 wavenumbers with a significant number of them having magnitudes

below $k = 1$. Run 7 has 540 wavenumbers with several in both wave-

number ranges.

The computing time necessary for a run varied from less than

2 minutes for Run 2 to approximately 1 hour for Run 7 on the MFE

CDC7600 computer. This drastic change in computing time is not only

because the system of equations is larger in Run 7 than in Run 2 but

also because of the nature of the equations themselves. Equations

(6)—(9) are examples of stiff differential equations.[16,17]

Typically one has a set of stiff differential equations whenever the

largest time scale in the problem is orders of magnitude larger than

the smallest time scale in the problem. Good numerical techniques

for stiff differential equations are one of the current frontiers in

numerical mathematics. Numerical methods which perform excellently

on non-stiff equations may fare poorly on stiff equations. Time steps

in many standard schemes must be chosen small enough to fit every time

scale in the problem even if the faster scales are transient. The

time step in our current problem was chosen to meet stability require-

ments; the time step was halved whenever the errors in the conserved

quantities indicated that numerical instabilities were beginning to

arise.

Time-averaged electric field energy spectra were computed at various intervals during the course of a run. The final time-averaged spectra are compared with the ensemble-averaged spectra in Eq. (31).

Figures 1, 2, and 3 show spectra for Runs 2, 3, and 7, respectively. Each of the three figures consists of three panels: panel (a) shows the initial spectrum; panel (b) shows a time-averaged spectrum during the middle of the run, and panel (c) shows the final time-averaged spectrum. The solid curve in panel (c) of each figure is the theoretical prediction. In Figure 1, panel (b) shows the spectrum for Run 2 averaged between times $t = 8.0$ and $t = 16.0$ while the spectrum in panel (c) is averaged between times $t = 24.0$ and $t = 32.0$. In Figure 2 the spectrum in panel (b) is averaged between times $t = 64.0$ and $t = 128.0$ and in panel (c) the spectrum is averaged between times $t = 192.0$ and $t = 256.0$ for Run 3. The times in Figure 3 for Run 7 are $t = 8.0$ and $t = 16.0$ for panel (b) and $t = 24.0$ and $t = 32.0$ for panel (c). Every wavenumber is plotted in Figures 1 and 2. Because the density of points in a logarithmic plot becomes so great at the high-k end of the spectrum for Run 7 only every other point is plotted for $3 < k < 10$ and every fourth point is plotted for $k > 10$ in Figure 3.

Time histories of two typical Fourier coefficients are shown in Figure 4 for Run 2. Figure 4(a) shows the real part of $n(k = 1)$, or equivalently the imaginary part of $E(k = 1)$, as a function of time. Figure 4(b) shows the real part of $n(k = 8)$, or equivalently the imaginary part of $8E(k = 8)$, as a function of time.

Figure 5 shows time histories of two Fourier coefficients for Run 3. Figure 5(a) shows the real part of $n(k = 1/16)$ vs. time and Figure 5(b) shows the real part of $n(k = 1/2)$ plotted against time.

In both Figures 4 and 5 the oscillations predicted by the linear theory seem to be present. A linear theory for Eqs. (6)—(9) gives, in our dimensionless units, the dispersion relation

$$\omega^2 = 1 + k^2 \tag{33}$$

relating the frequency ω to the wavenumber k. For $k = 1/16$ this relation gives a period $T = 2\pi/\omega \simeq 6.1$. Counting peaks in Figure 5(a) and dividing into the total time interval between the first and last peak gives $T \simeq 6.2$. A similar calculation for $k = 1/2$ gives a theoretical period of $T \simeq 5.6$ and from Figure 5(b) $T \simeq 5.8$; for $k = 1$ the theoretical period is $T \simeq 4.4$ and from Figure 4(a) $T \simeq 4.1$; for $k = 8$ the theoretical period is $T \simeq 0.785$ while from Figure 4(b) $T \simeq 0.778$. It appears that the linear oscillations are present but that clearly something else is happening as well.

Figure 6 shows the electric field energy as a function of time for the two modes of Run 2 shown in Figure 4. Figure 6(a) shows $|E(k = 1)|^2$ versus time and Figure 6(b) shows $|E(k = 8)|^2$ versus time. One should notice the orders of magnitude variation in the amplitudes of the modal energies. Because of this a time instantaneous wavenumber spectrum has considerably more scatter in the points compared

to the time-averaged spectra of Figures 1—3. The time history plots
also show the more rapid flow of energy into and out of the higher
modes. This can be expected from Eqs. (6)—(8) where we can see the
the terms responsible for this energy transfer are proportional to
the wavenumber itself. Not only do the higher wavenumber Fourier
coefficients oscillate on a more rapid time scale but they also
equilibrate faster as indicated by the spectral plots in Figures 1—3.
This fast rush of energy to the large wavenumbers and hence smaller
spatial scales would indicate the possibility for shock formation.

Figures 7, 8, and 9 show configuration space plots of number
density, velocity, and electric field, respectively, at four various
times in the course of Run 7. The shock formation is most clear in
the velocity profiles of Figure 8. Initially the velocity is zero.
The first thing to occur is the linear transfer of energy from the
electric and pressure fields to kinetic energy. At this point the
nonlinear term in Eq. (7) begins to have effect. A simple analysis
of the equation

$$\frac{\partial v}{\partial t} + v \frac{\partial v}{\partial x} = 0 \tag{34}$$

shows that discontinuities form in a finite time. The time to this
discontinuity given the data of Figure 8 at time $t = 0.5$ predicts the
discontinuity to form at time $t = 1.7$, later than the profiles indicate.
The fact that something drastic has happened is even more clear in the

last density profile of Figure 7 in which the plot is virtually up
and down between grid points. Beyond time $t = 1.0$ the configuration
space profiles cannot mean much. This does not mean that the numeri-
cal solutions of Eqs. (6)—(9) are incorrect or that the computed
spectra of Figures 1—3 are mathematically wrong. Because the time
to discontinuity is much shorter than the time to equilibrium means
only that the truncated Fourier representation in Eqs. (6)—(9) is
no longer an adequate approximation to the continuous Eqs. (1)—(4)
in the non-dissipative limit. We expect that with the addition of a
finite dissipation at high wavenumbers that the discontinuities will
not occur. If enough grid points are used (and hence more modes
are kept in the truncation) we expect to be able to determine a shock
width and the truncated Fourier equations will be adequate for very
long times. The spectral laws may be different for the dissipative
problem than they are here for the non-dissipative one just as the
dissipative problem is significantly different from the non-dissipative
one in Navier-Stokes fluids and MHD. What the above calculations do
seem to indicate is that migrations of energy over large spatial
scales is possible in a one-dimensional electron fluid. Any accurate
assertions involving turbulent electron plasma oscillations must take
these migrations into account.

V. DISCUSSION

In the previous sections we have produced a statistical mechanical description for turbulent motions in a one-dimensional electron fluid plasma. The prominent aspect of this paper is the application of the techniques of fluid turbulence to a compressible situation. Much needs to be done, however, before applications to physical systems can be considered. The first obvious generalization is the addition of a finite dissipation to the problem. Dissipation will undoubtedly alter the results here as it has in the analysis of other fluid equations. For example, Kolmogoroff arguments postulating an energy cascade would lead to $|E(k)|^2 \sim k^{-5/3}$. Although migrations of energy across many length scales seems likely in this dissipative problem, it is unclear at this point whether the transfer of energy will be able to produce large scale electric fields through some sort of inverse cascade process, and there is no suggestion of them in the theory thus far. Shocks are also likely to play some role in this problem.

Along other lines the inclusion of mobile ions could have unknown effects. Extensions to multiple space dimensions could also produce a variety of results. We already know that two-dimensional Navier-Stokes and MHD fluids behave differently from their three-dimensional counterparts. It is not inconceivable that a

multi-dimension electron fluid plasma may behave differently than the one-dimensional plasma studied here.

We are also aware that Langmuir turbulence spectra which fall off as k^{-2} at large k·have arisen in simulations far more complex than this one (see, e.g., Thomson et al.[18]) and may result from a variety of arguments. We refrain from speculating as to whether the k^{-2} behavior should characterize either (1) mobile ion situations, or (2) situations with finite dissipation.

ACKNOWLEDGMENTS

We would like to thank G. R. Joyce for his comments. One of us (D.F.) would also like to thank K. E. Atkinson for some enlightening discussions.

This work was supported by NASA Grant NGL-16-001-043 and USERDA Grant E(11-1)-2059.

APPENDIX A

Frequently in studies of fluid equations via plane wave expansions the $k = 0$ mode is neglected. The $k = 0$ Fourier coefficient can be thought of as the mean value per unit length of the quantity under discussion. For example

$$E(k = 0) = \frac{1}{2L} \int_0^L E(x) \, dx$$

$$n(k = 0) = \frac{1}{2L} \int_0^L n(x) \, dx$$

That the $E(k = 0)$ mode cannot be automatically set to zero can be illustrated in the following example. Suppose we were to start our electron fluid initially with no number density fluctuations. Then

$$E(x) = \int^x [1 - n(x)] \, dx$$

implies that $E(k = 0) = 0$. Assume also that the initial velocity fluctuations are such to produce at a later time a surplus of electrons in one region and a deficit of electrons in another, maintaining overall charge neutrality. (See Figure 10.) $E(x)$ in the situation depicted in Figure 10 no longer has an average value of

zero and hence $E(k = 0) \neq 0$. $E(k = 0)$ is just the jump in the scalar potential across one periodicity length, and periodic electric fields do not imply its vanishing. It is true that there are situations in which $E(k = 0)$ remains zero for all time, but these are not the most general situations one can envision.

APPENDIX B

In previous applications of truncated Fourier series to Navier-
Stokes or MHD fluids the conserved quantities are all quadratic in
the Fourier coefficients. In this appendix we will demonstrate the
conservation of ε in Eq. (10) which involves products of three Fourier
coefficients. There are four terms in ε: the triples, the remaining
kinetic energy, the mechanical energy associated with the pressure
field, and the electric field energy. We will differentiate each of
the four terms, apply Eqs. (6)—(8) and sum the results. For this
purpose it is helpful to rewrite Eqs. (6)—(8) in the form

$$\frac{\partial n(k)}{\partial t} = -ik \sum_{pr \neq 0} \delta(p + r - k)\, n(p)\, v(r) - ikv(k) - ikv(0)\, n(k) \quad ,$$

$$\tag{B1}$$

$$\frac{\partial v(k)}{\partial t} = -i\,\frac{k}{2} \sum_{pr \neq 0} \delta(p + r - k)\, v(p)\, v(r) - ikv(0)\, v(k)$$

$$- ikn(k) - \frac{i}{k}\, n(k) \tag{B2}$$

where we have separated all terms with zero wavenumber coefficients
and eliminated $E(k)$ in favor of $n(k)$ for $k \neq 0$. $\delta(p + r - k)$ is the

Kronecker delta which has the value 1 whenever its argument vanishes and the value 0 otherwise. Differentiating the triples we obtain

$$\frac{1}{2} \sum_{k_1 k_2 k_3 \neq 0} \delta(k_1 + k_2 + k_3) \left[n(k_1) \, v(k_2) \, \frac{\partial v(k_3)}{\partial t} \right.$$

$$\left. + n(k_1) \, v(k_3) \, \frac{\partial v(k_2)}{\partial t} + v(k_2) \, v(k_3) \, \frac{\partial n(k_1)}{\partial t} \right] \quad .$$

Since the labels by which we refer to wavenumbers is immaterial, we notice that with the interchange of the labels k_2 and k_3 in the second term that it is identical to the first term. Consequently, after applying Eqs. (B1) and (B2) we obtain

$$\frac{\partial}{\partial t} \, (\text{triples})$$

$$= \sum_{k_1 k_2 k_3 \neq 0} \delta(k_1 + k_2 + k_3) \, n(k_1) \, v(k_2)$$

$$\times \left[-\frac{ik_3}{2} \sum_{pr \neq 0} \delta(p + r - k_3) \, v(p) \, v(r) - ik_3 v(0) \, v(k_3) \right.$$

$$\left. - ik_3 \, n(k_3) - \frac{1}{k_3} \, n(k_3) \right]$$

$$+ \frac{1}{2} \sum_{k_1 k_2 k_3 \neq 0} \delta(k_1 + k_2 + k_3) \, v(k_2) \, v(k_3)$$

$$\times \left[-ik_1 \sum_{pr \neq 0} \delta(p + r - k_1) \, n(p) \, v(r) \right.$$

$$\left. - ik_1 v(k_1) - ik_1 n(k_1) v(0) \right] \tag{B3}$$

which consists of seven terms. In the first term we sum over k_3. Again since the labels by which we refer to wavenumbers is immaterial, after we have summed over k_3 we replace the labels p and r with the labels k_3 and k_4. In the fifth term, which also involves four Fourier coefficients, after we have summed over k_1 we replace p and r with k_1 and k_4, respectively. The result for those two terms is

$$\frac{1}{2} \sum_{k_1 k_2 k_3 k_4 \neq 0} \delta(k_1 + k_2 + k_3 + k_4) \, n(k_1) \, v(k_2) \, v(k_3) \, v(k_4) \, i(k_3 + k_4)$$

$$+ \frac{1}{2} \sum_{k_1 k_2 k_3 k_4 \neq 0} \delta(k_1 + k_2 + k_3 + k_4) \, n(k_1) \, v(k_2) \, v(k_3) \, v(k_4) \, i(k_1 + k_4) \; .$$

In the last term we may exchange the label k_4 with the label k_2. The resulting overall sum of these terms with factors $n(k_1) \, v(k_2) \, v(k_3) \, v(k_4)$ contains a factor $(k_1 + k_2 + k_3 + k_4) \, \delta(k_1 + k_2 + k_3 + k_4)$ which

always vanishes. Hence the first and fifth terms of (B3) cancel.

In a similar way the second and seventh terms of (B3) cancel; their sum is

$$-\frac{1}{2} \sum_{k_1 k_2 k_3 \neq 0} \delta(k_1 + k_2 + k_3)\, n(k_1)\, \dot v(k_2)\, v(k_3)\, v(0)\, (k_1 + 2k_3) \quad .$$

Again exchange one k_3 for a k_2 to obtain a factor $(k_1 + k_2 + k_3)$ $\delta(k_1 + k_2 + k_3)$ which always vanishes. The sixth term, after cyclic permutations of wavenumbers $k_1 \to k_2 \to k_3$, can be written as

$$-\frac{1}{2} \sum_{k_1 k_2 k_3 \neq 0} \delta(k_1 + k_2 + k_3)\, v(k_2)\, v(k_3)\, ik_1 \dot v(k_1)$$

$$= -\frac{1}{6} \sum_{k_1 k_2 k_3 \neq 0} \delta(k_1 + k_2 + k_3)\, i(k_1 + k_2 + k_3)\, \dot v(k_1)\, v(k_2)\, v(k_3)$$

which also vanishes. Hence in summary

$$\frac{\partial}{\partial t}(\text{triples}) = -i \sum_{k_1 k_2 k_3 \neq 0} \delta(k_1 + k_2 + k_3)\, n(k_1)\, v(k_2)\, n(k_3)\left(k_3 + \frac{1}{k_3}\right) \quad .$$

$$\text{(B4)}$$

Differentiating the remaining kinetic energy terms of $\mathcal{E}$ gives by a similar process

$$\frac{\partial}{\partial t}\left[\frac{1}{2}\sum_{k\neq 0}|v(k)|^2\right] = \sum_{k\neq 0}v(-k)\,\frac{\partial v(k)}{\partial t}$$

$$= \sum_{k\neq 0}v(-k)\left[-\frac{ik}{2}\sum_{pr\neq 0}\delta(p+r-k)\,v(p)\,v(r)\right.$$

$$\left. - ikv(0)\,v(k) - ikn(k) - \frac{i}{k}\,n(k)\right]$$

$$= -i\sum_{k\neq 0}n(k)\,v(-k)\left(k+\frac{1}{k}\right) \quad . \qquad (B5)$$

Differentiating the pressure terms gives

$$\frac{\partial}{\partial t}\left[\frac{1}{2}\sum_{k\neq 0}|n(k)|^2\right] = \sum_{k\neq 0}n(-k)\,\frac{\partial n(k)}{\partial t}$$

$$= \sum_{k\neq 0}n(-k)\left[-ik\sum_{pr\neq 0}\delta(p+r-k)\,n(p)\,v(r)\right.$$

$$\left. - ikv(k) - ikv(0)\,n(k)\right]$$

$$= i\sum_{k_1 k_2 k_3\neq 0}\delta(k_1+k_2+k_3)\,n(k_1)\,v(k_2)\,n(k_3)\,k_3$$

$$+ i\sum_{k\neq 0}n(k)\,v(-k)\,k \quad . \qquad (B6)$$

And finally the electric field energy terms give

$$\frac{\partial}{\partial t}\left[\frac{1}{2}\sum_k |E(k)|^2\right] = \frac{\partial}{\partial t}\left[\frac{1}{2}\sum_{k\neq 0}\frac{|n(k)|^2}{k^2}\right]$$

$$= \sum_{k\neq 0}\frac{n(-k)}{k^2}\left[-ik\sum_{pr\neq 0}\delta(p+r-k)\,n(p)\,v(r)\right.$$

$$\left. - ikv(k) - ikv(0)\,n(k)\right]$$

$$= i\sum_{k_1 k_2 k_3\neq 0}\delta(k_1+k_2+k_3)\,n(k_1)\,v(k_2)\,n(k_3)\frac{1}{k_3}$$

$$+ i\sum_{k\neq 0}n(k)\,v(-k)\frac{1}{k} \quad . \tag{B7}$$

Summing Eqs. (B4)—(B7) then gives $\partial\mathscr{E}/\partial t = 0$. $\partial J/\partial t = 0$ can be proven in a similar manner.

Table I

List of Parameters for Three Typical
Numerical Calculations

	Run 2	Run 3	Run 7
N (number of grid points)	64	64	512
L (length of system in 2_D)	2π	32π	16π
$k_{min} = 2\pi/L$	1	1/16	1/8
k_{max}	21	21/16	170/8
Size of time step	$(64)^{-1}$	$(64)^{-1}$	$(512)^{-1}$ $(1024)^{-1}$
Duration of run (in ω_{pe}^{-1})	32.	256.	32.
Initial non-zero velocity coefficients	None	None	None
Initial non-zero density (electric field) coefficients	$k = 6, 7, 8, 9, 10$	$k = 6/16, 7/16, 8/16, 9/16, 10/16$	$k = 6/8, 7/8, 8/8, 9/8, 10/8$
Initial ε Final ε Percent change in ε	0.134 0.135 6.67×10^{-3}	0.644 0.644 2.1×10^{-6}	0.260 0.260 8.2×10^{-6}
Initial J Final J	0 -3.3×10^{-5}	0 -1.2×10^{-8}	0 8.7×10^{-8}
Initial Q Final Q	0 1.5×10^{-9}	0 4.3×10^{-15}	0 -5.0×10^{-15}
α	0.00336	0.0173	0.0009
Triples at end of run	-0.004	-0.055	-0.014

REFERENCES

[1] U. Frisch, A. Pouquet, J. Leorat, and A. Mazure, J. Fluid Mech. 68, 769 (1975).

[2] A. Pouquet, U. Frisch, and J. Leorat, J. Fluid Mech. 77, 321 (1976).

[3] A. Pouquet and G. S. Patterson, Jr., "Numerical Simulation of Helical Magnetohydrodynamic Turbulence", NCAR Preprint (1976).

[4] D. Fyfe and D. Montgomery, J. Plasma Phys. 16, 181 (1976).

[5] D. Fyfe, G. Joyce, and D. Montgomery, J. Plasma Phys. 17, 317 (1977).

[6] D. Fyfe, D. Montgomery, and G. Joyce, "Dissipative, Forced Turbulence in Two-dimensional Magnetohydrodynamics", to be published in J. Plasma Phys. (1977).

[7] A. Pouquet, "On Two Dimensional Magnetohydrodynamic Turbulence", Observatoire de Nice preprint (1977).

[8] S. A. Orszag, Stud. Appl. Math. 50, 293 (1971).

[9] G. S. Patterson, Jr. and S. A. Orszag, Phys. Fluids 14, 2358 (1971).

[10] Y. Salu and G. Knorr, J. Comp. Phys. 17, 68 (1975).

[11] C. E. Seyler, Jr., Y. Salu, D. Montgomery, and G. Knorr, Phys. Fluids 18, 803 (1975).

[12] J. D. Cole, Quart. of Applied Math. 9, 225 (1951).

[13] J. M. Burgers, in Statistical Models and Turbulence, ed. by M. Rosenblatt and C. van Atta (Springer-Verlag, New York, 1972).

[14] K. M. Case, in Statistical Models and Turbulence, ed. by M. Rosenblatt and C. van Atta (Spring-Verlag, New York, 1972).

[15] T. D. Lee, Quart. Appl. Math. $\underline{10}$, 69 (1952).

[16] C. W. Gear, Numerical Initial Value Problems in Ordinary Differential Equations (Prentice Hall, Englewood Cliffs, New Jersey, 1971).

[17] Modern Numerical Methods for Ordinary Differential Equations, ed. by G. Hall and J. M. Watt (Clarendon Press, Oxford, 1976).

[18] J. J. Thomson, R. J. Faehl, W. L. Kruer, and S. Bodner, Phys. Fluids $\underline{17}$, 973 (1974).

FIGURE CAPTIONS

Fig. 1   Electric field energy spectra $|E(k)|^2$ vs. k for Run 2:

(a) initial conditions; (b) time averaged over times t = 8.0

to 16.0; (c) time averaged over times t = 24.0 to 32.0.

Theoretical curve is the solid line in Fig. 1(c).

Fig. 2   Electric field energy spectra $|E(k)|^2$ vs. k for Run 3:

(a) initial conditions; (b) time averaged over times

-t = 64.0 to 128.0; (c) time averaged over times t = 192.0

to 256.0.   Theoretical curve is the solid line in Fig. 2(c).

Fig. 3   Electric field energy spectra $|E(k)|^2$ vs. k for Run 7:

(a) initial conditions; (b) time averaged over times

t = 8.0 to 16.0; (c) time averaged over times t = 24.0

to 32.0.   Theoretical curve is the solid line in Fig. 3(c).

For clarity, only every other value of k is plotted for

3 < k < 10 and every fourth value for k > 10.

Fig. 4   Time histories of two typical Fourier coefficients in Run 2:

(a) the real part of n(k = 1, t); (b) the real part of

n(k = 8, t).

Fig. 5   Time histories of two typical Fourier coefficients in Run 3:

(a) the real part of n(k = 1/16, t); (b) the real part of

n(k = 1/2, t).

Fig. 6   Time histories of electric field energies for two modes in Run 2:   (a) $|E(k = 1, t)|^2$, (b) $|E(k = 8, t)|^2$.

Fig. 7   Number density profiles at four different times in the evolution of Run 7.

Fig. 8   Velocity field profiles at four different times in the evolution of Run 7.

Fig. 9   Electric field profiles at four different times in the evolution of Run 7.

Fig. 10   Illustration showing the necessity for the $E(k = 0)$ Fourier coefficient.   The top graphs show the initial $n(x)$ and $E(x)$ with $E(k = 0) = 0$.   The bottom graphs show the final $n(x)$ and $E(x)$ with $E(k = 0) \neq 0$.

Figure 1

$$\langle \, |E(k)|^2 \rangle$$

k
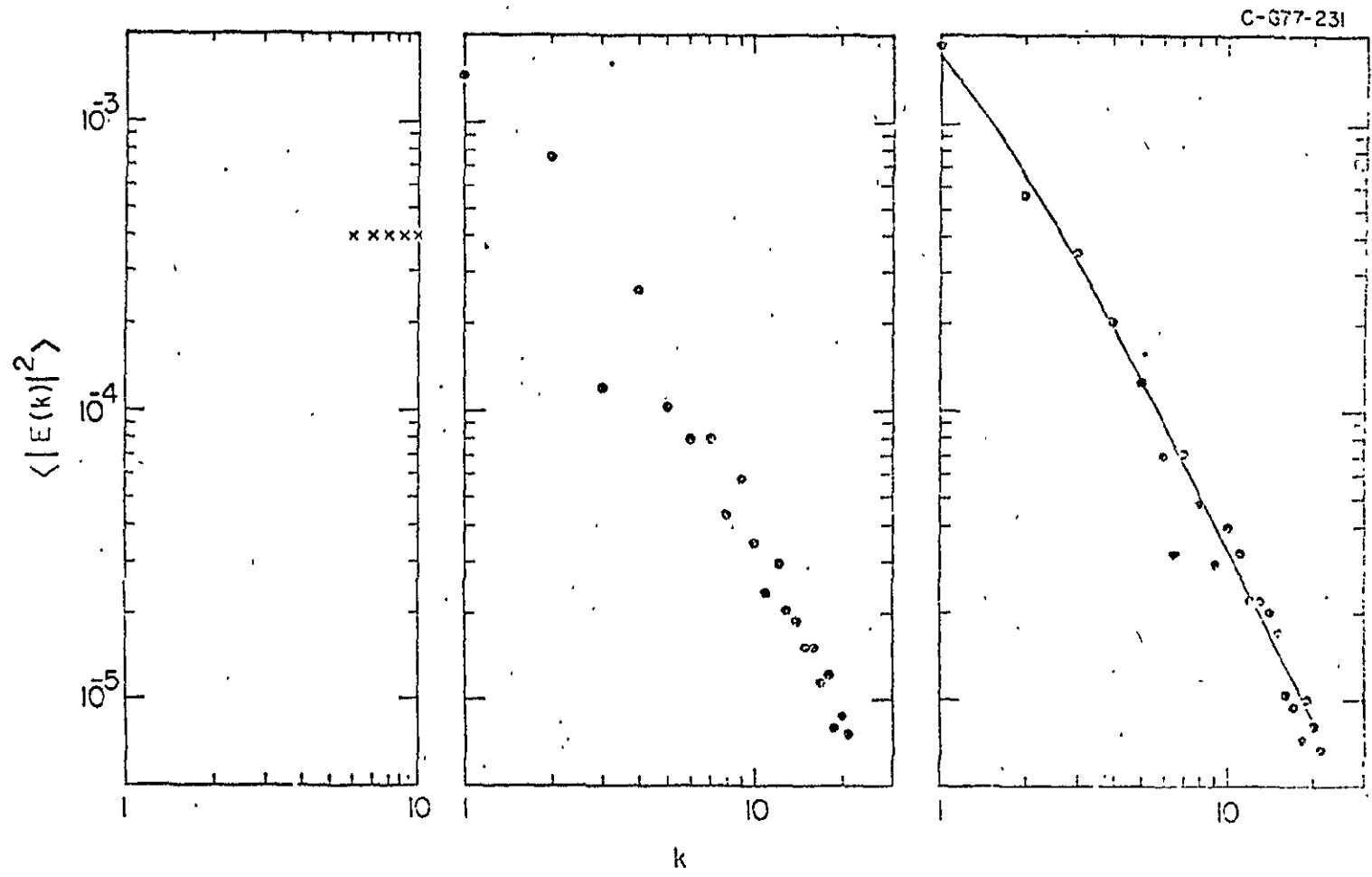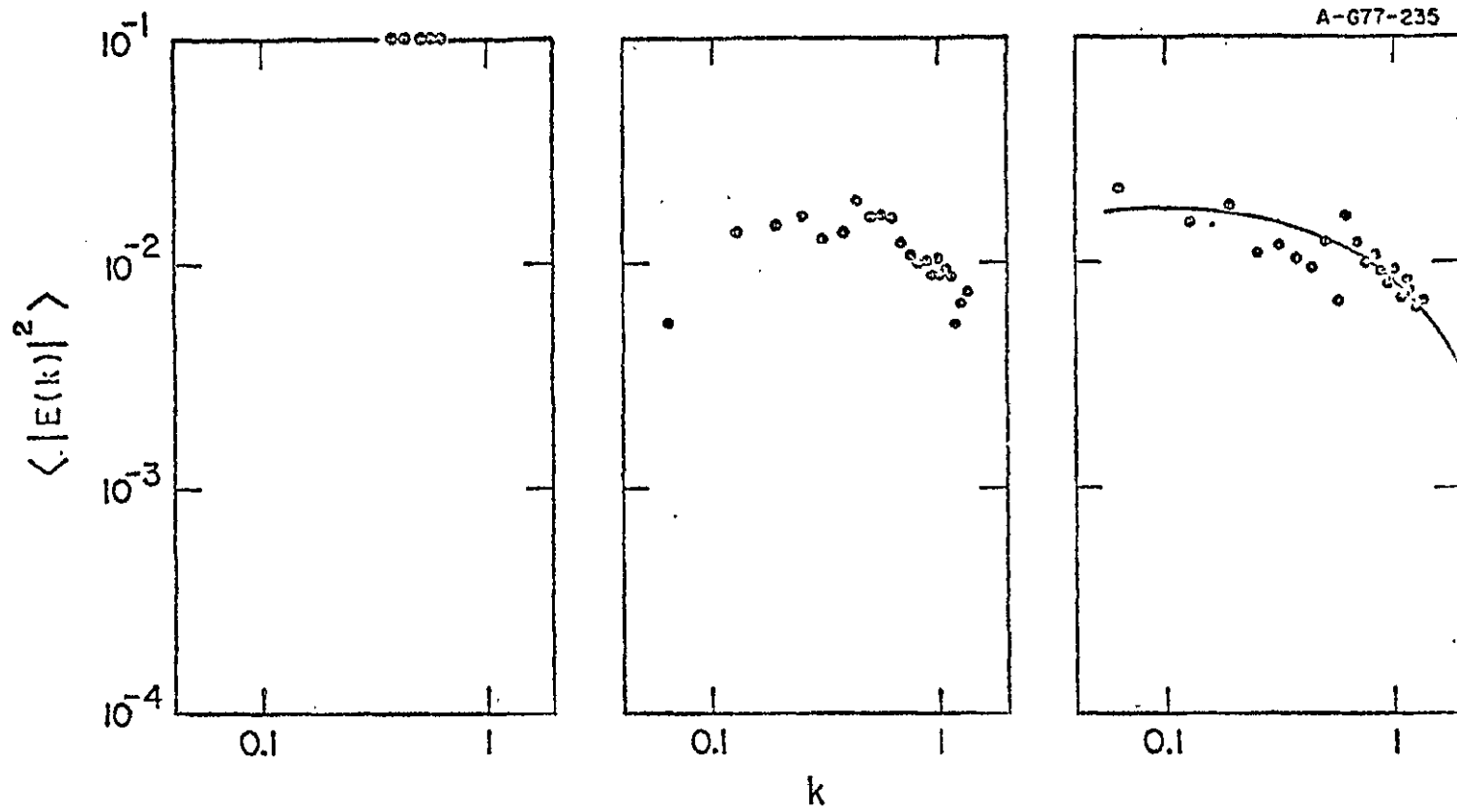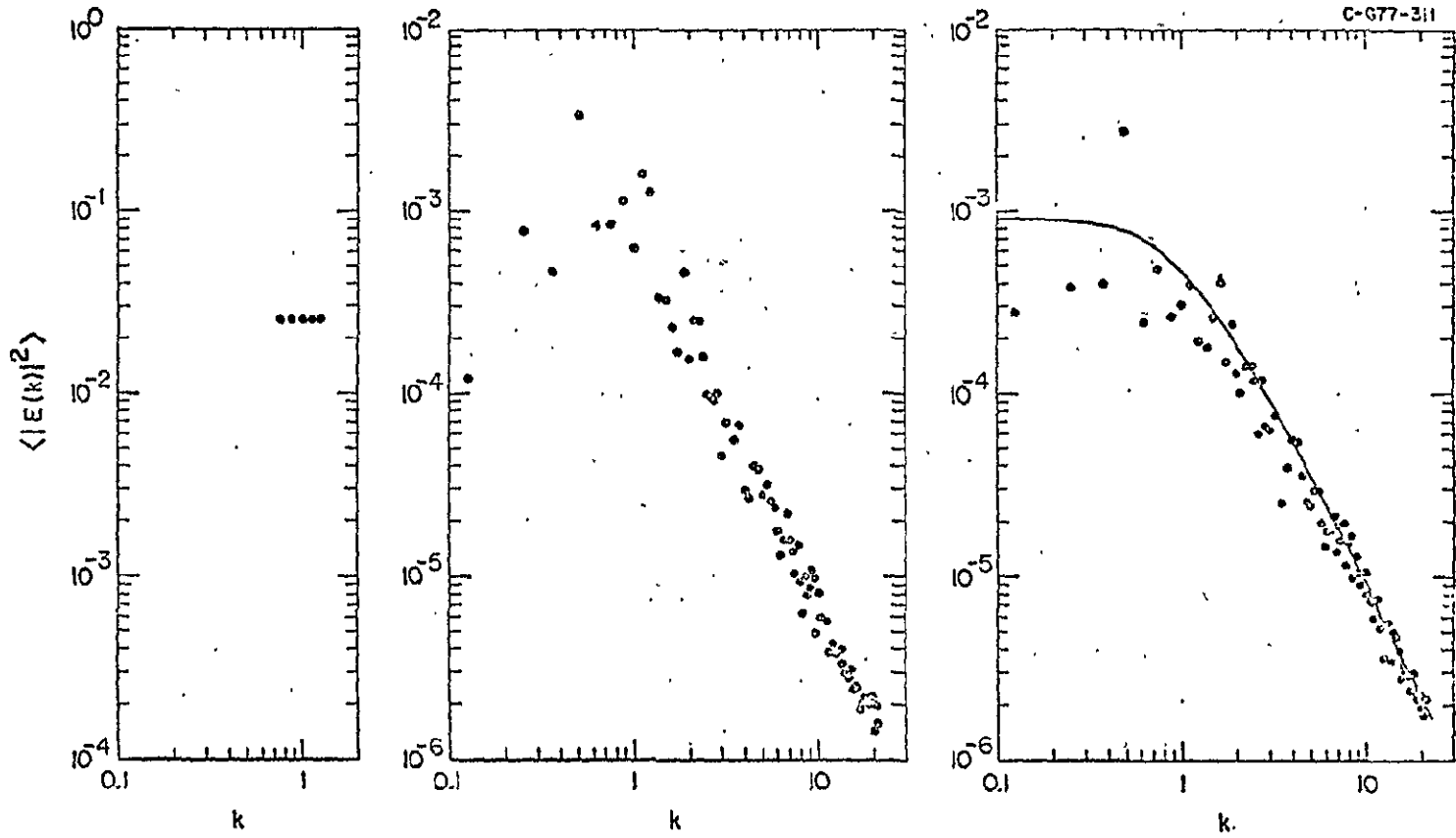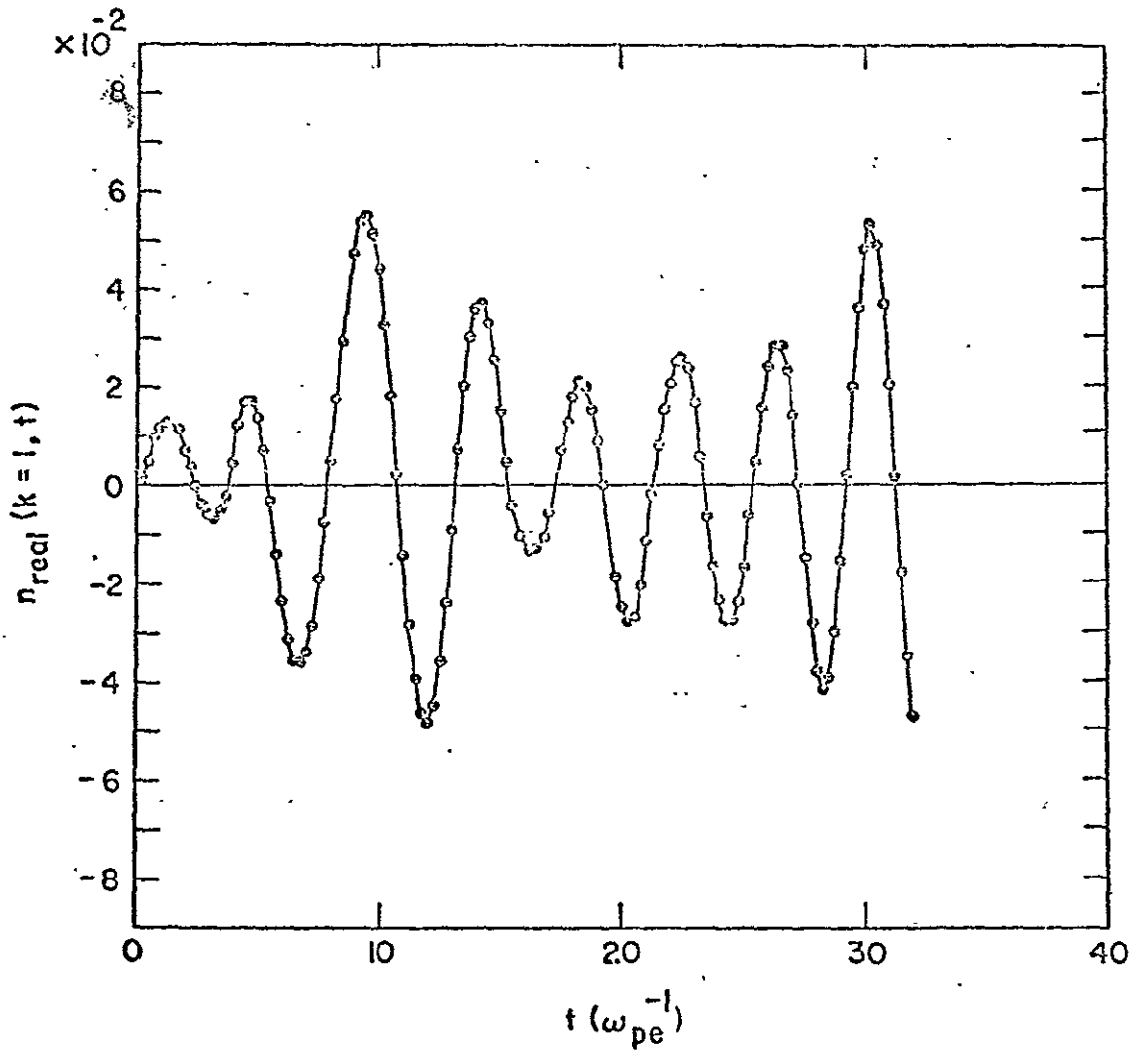
Figure 2

Figure 3

Figure 4(a)
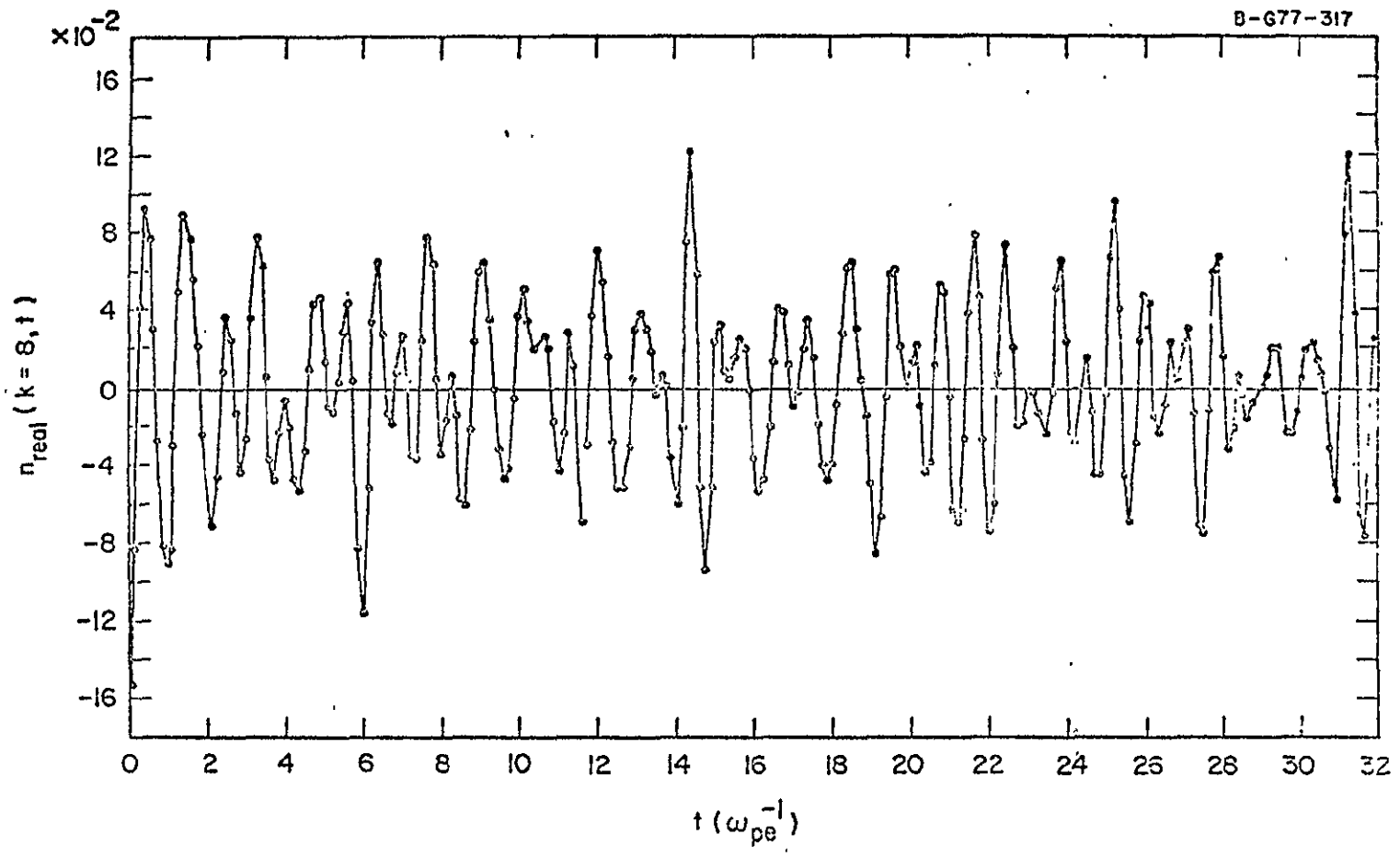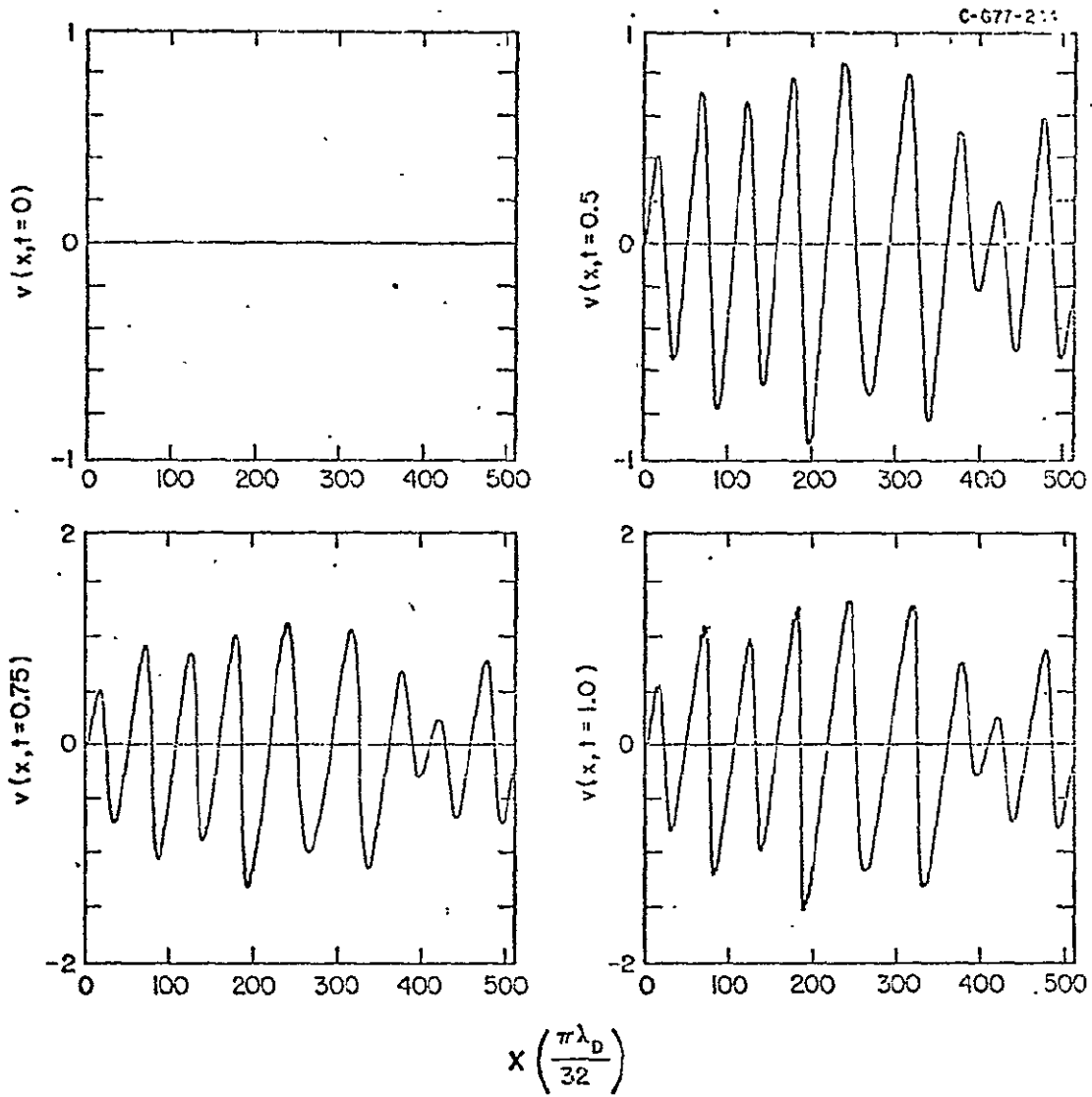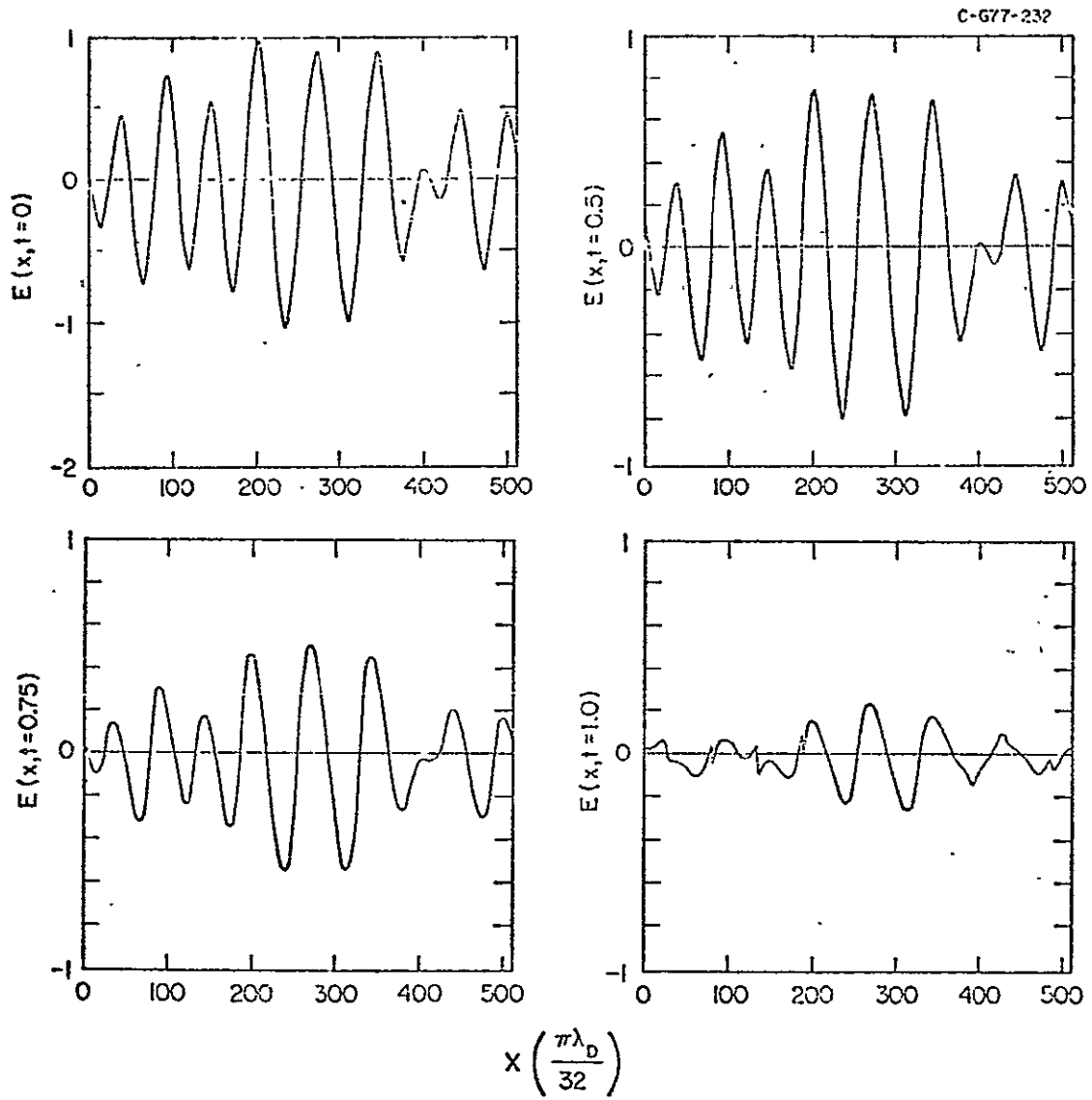
Figure 4(b)
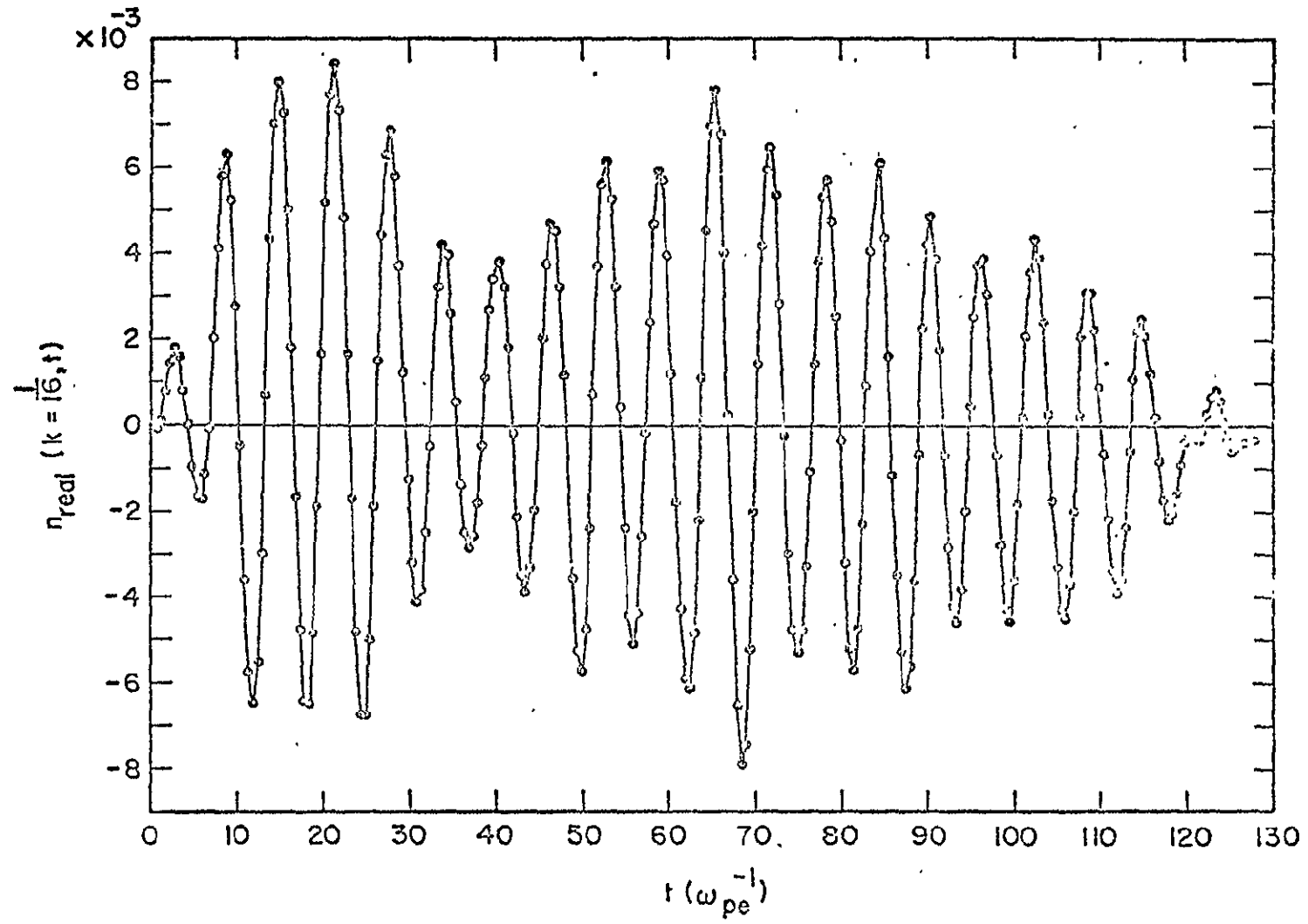
Figure 5(a)
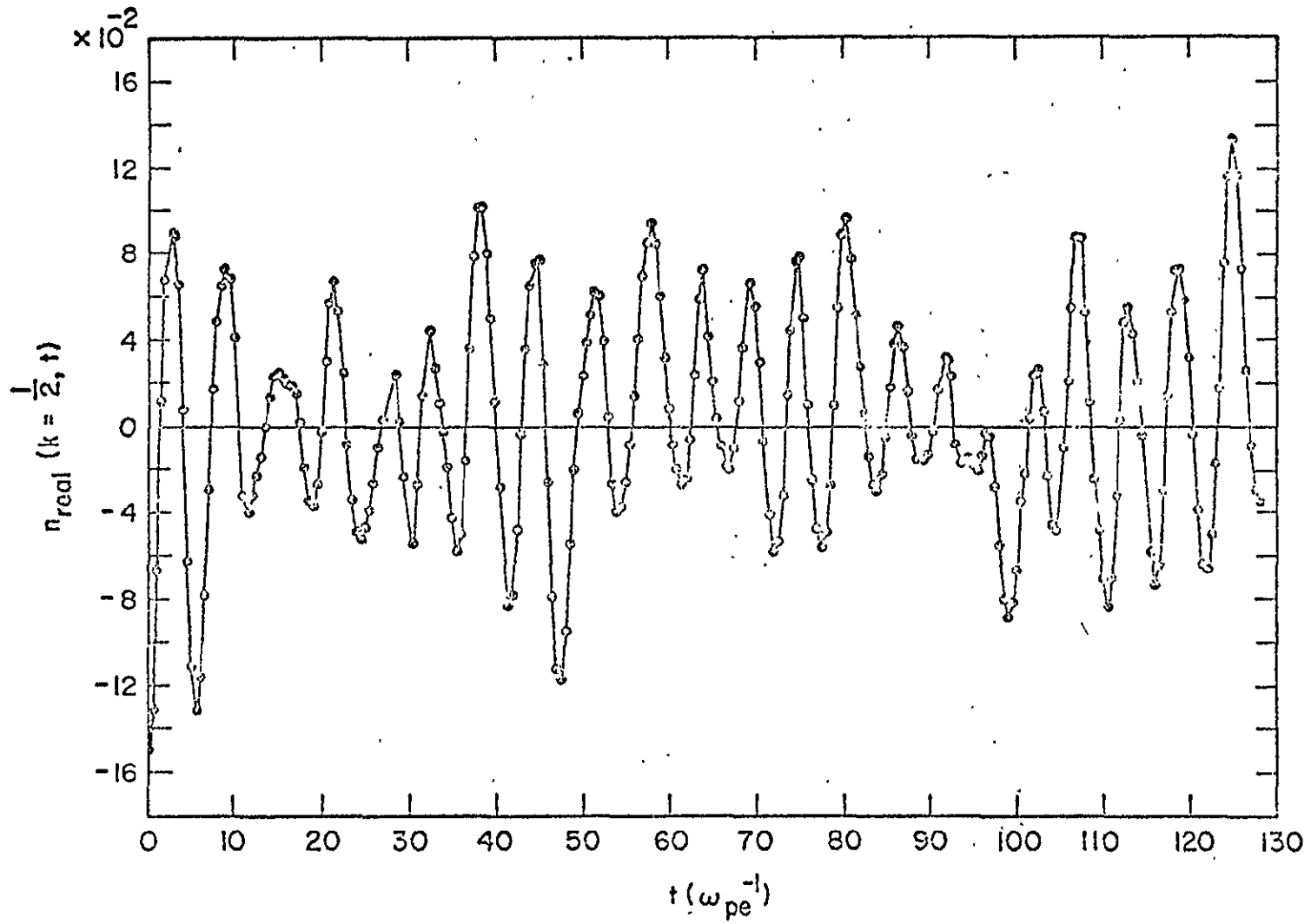
Figure 5(b)
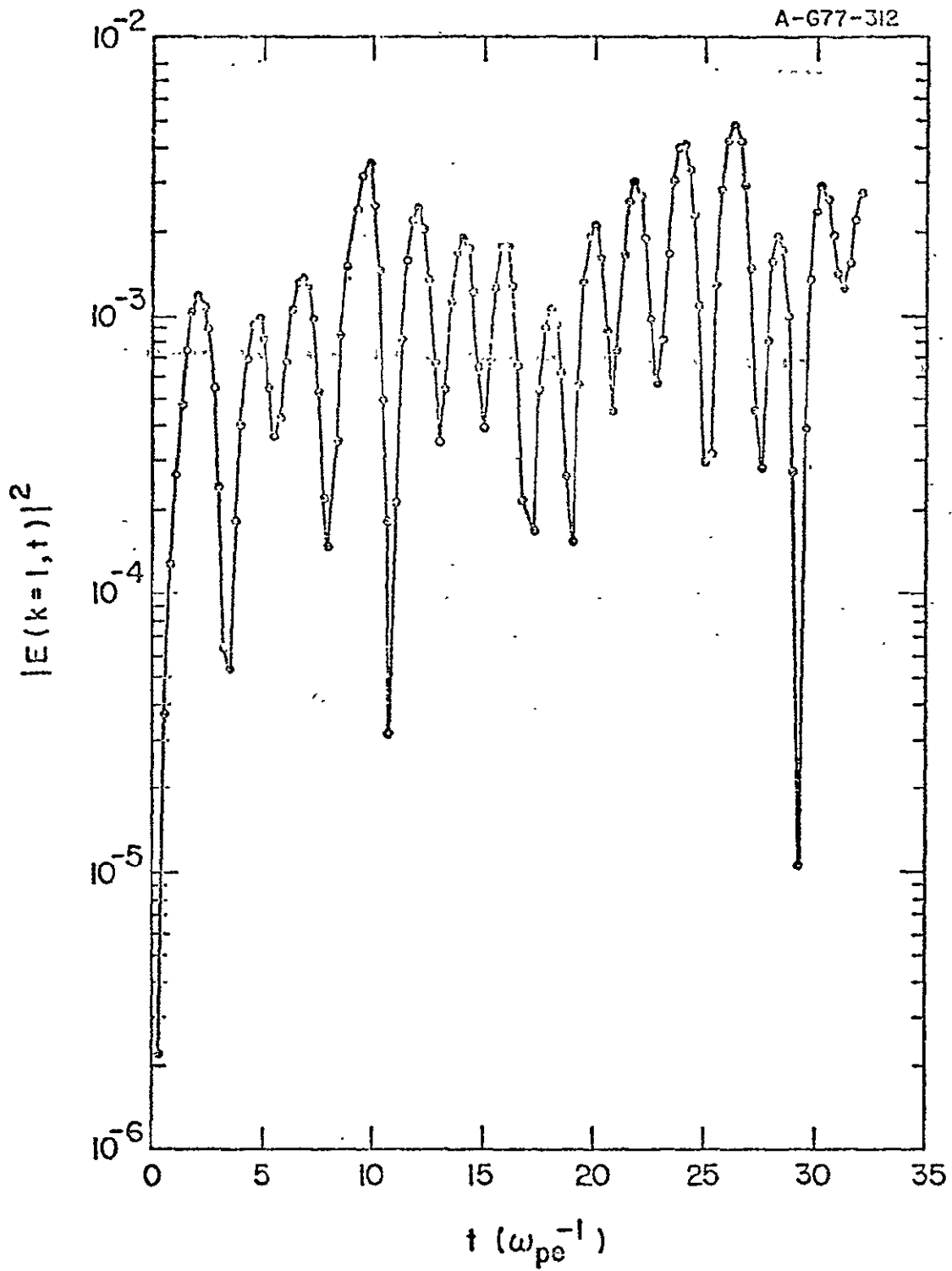
Figure 6(a)
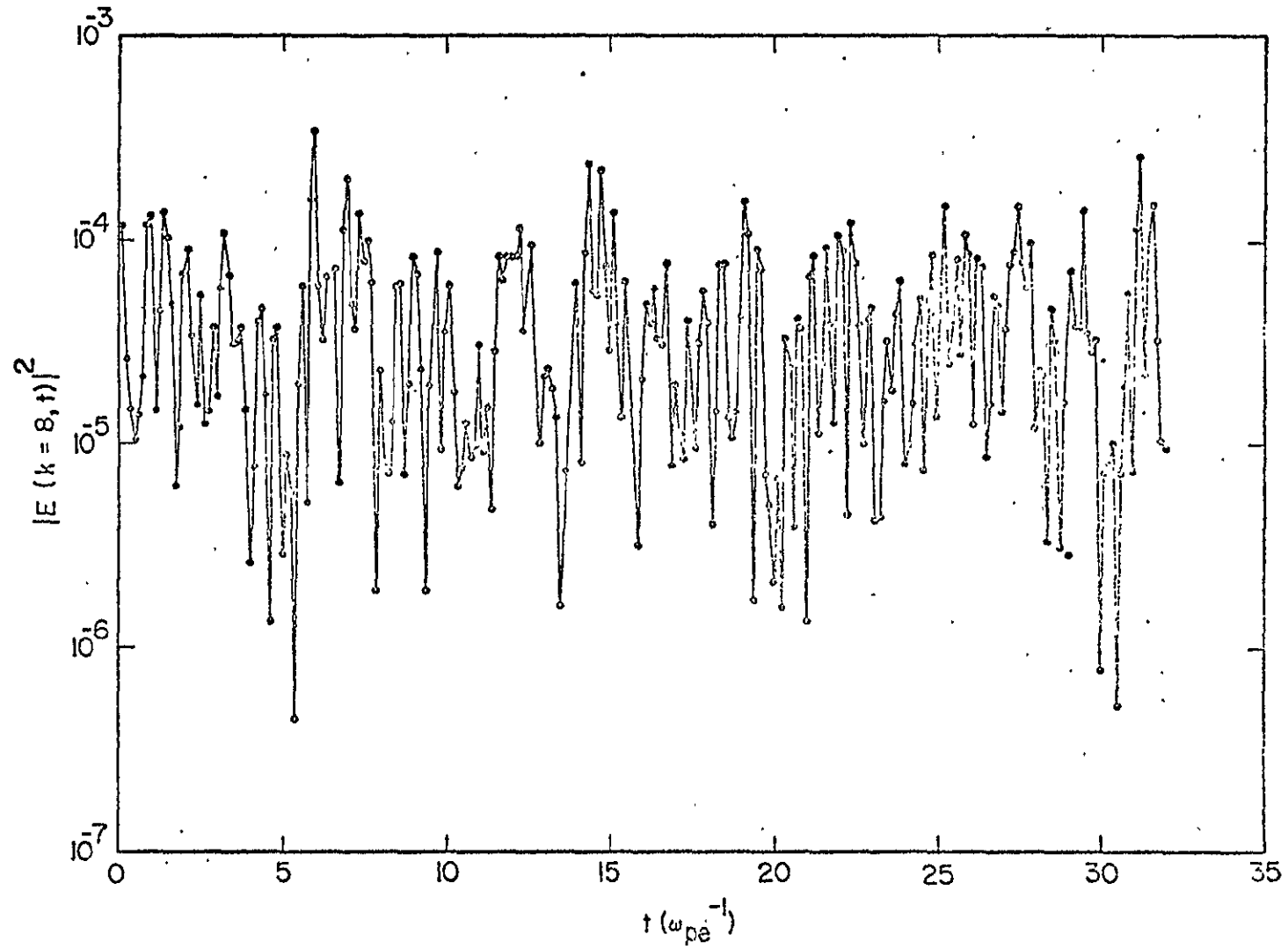
Figure 6(b)
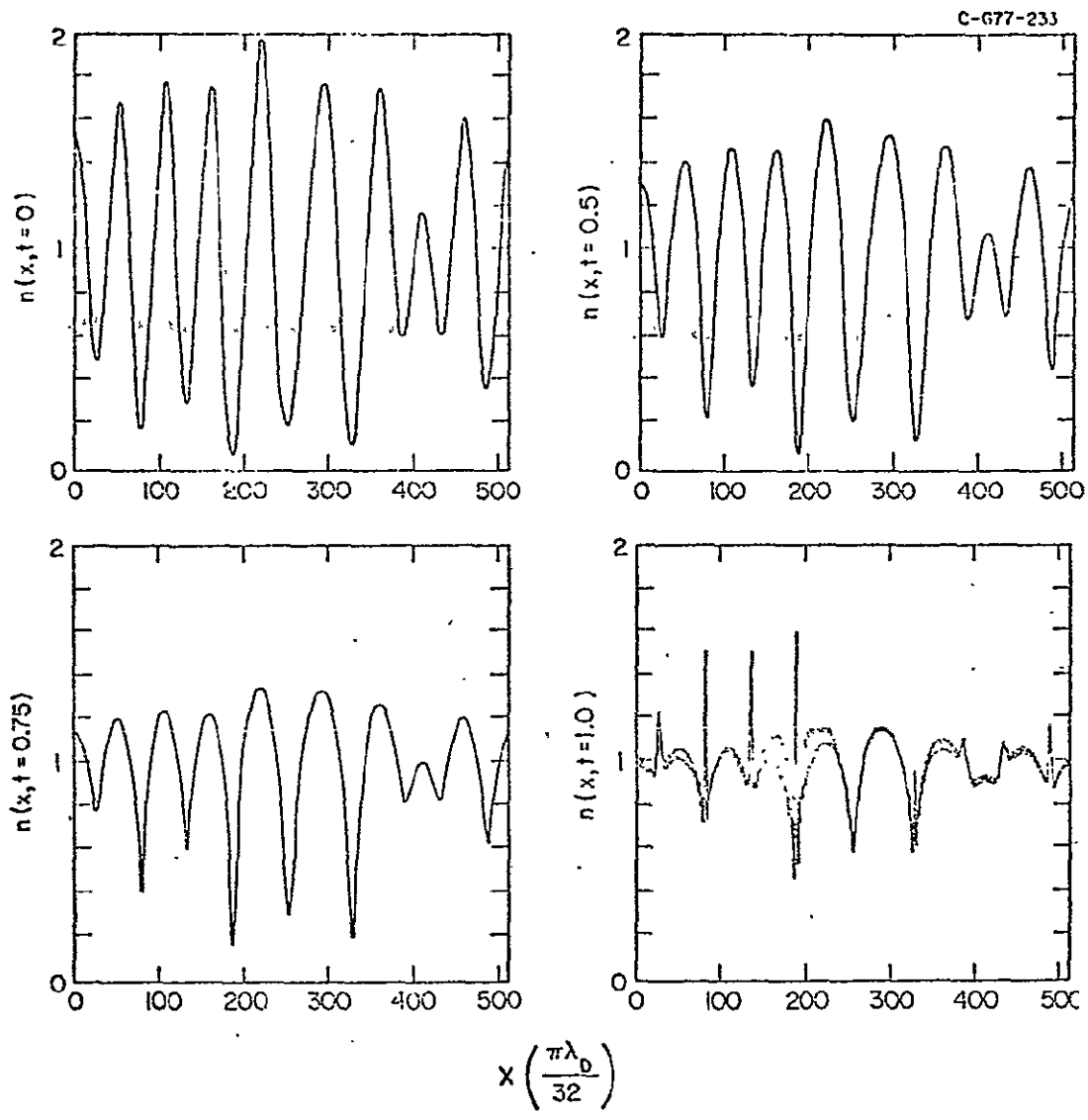
Figure 7

Figure 8

Figure 9

Figure 10